Engineered Disulfide Bonds in Staphylococcal Nuclease: Effects on the Stability and Conformation of the Folded Protein†

Andrew P. Hinck,‡ Dagmar M. Truckses, and John L. Markley*

Department of Biochemistry, 420 Henry Mall, University of Wisconsin, Madison, Wisconsin 53706

Received February 8, 1996; Revised Manuscript Received May 20, 1996⊗

ABSTRACT: Efforts to enhance the stability of proteins by introducing engineered disulfide bonds have resulted in mixed success. Most approaches to the prediction of the energetic consequences of disulfide bond formation in proteins have considered only the destabilizing effects of cross-links on the unfolded state (chain entropy model) [Pace, C. N., Grimsley, G. R., Thomson, J. A., & Barnett, B. J. (1988) *J. Biol. Chem. 263*, 11820−11825; Doig, A. J., & Williams, D. H. (1991) *J. Mol. Biol. 217*, 389−398]. It seems clear, however, that disulfide bridges also can influence the stability of the native state. In order to assess the importance of the latter effect, we have studied four variants of staphylococcal nuclease (V8 strain) each containing one potential disulfide bridge created by changing two wild-type residues to cysteines by site-directed mutagenesis. In each case, one of the introduced cysteines was within the type VI_a β turn containing *cis* Pro^{117}, and the other was located in the adjacent extended loop containing Gly^{79}. In all four cases, the overall loop size was kept nearly constant (the number of residues in the loop between the two cysteines varied from 37 to 42) so as to minimize differences from chain entropy effects. The objective was to create variants in which a change in the reduction state of the disulfide would be coupled to a change in the position of the equilibrium between the *cis* and *trans* forms of the Xxx^{116}−Pro^{117} peptide bond in the folded state of the protein. The position of this equilibrium, which can be detected by NMR spectroscopy, has been shown previously to correlate with the stability of the native protein. Its determination provides a measure of strain in the folded state. The thermal stabilities and free energies for unfolding by elevated temperature and guanidinium chloride were measured for each of the four mutants under conditions in which the introduced cysteines were cross-linked (oxidized) and unlinked (reduced). In addition, reduction potentials were determined for each mutant. Formation of the different disulfide bridges was found to induce varying levels of folded state strain. The stabilization energy of a given disulfide bridge could be predicted from the measured perturbation energy for the peptide bond isomerization, provided that energetic effects on the unfolded state were calculated according to the chain entropy model. Undiagnosed strain in native states of proteins may explain the variability observed in the stabilization provided by engineered disulfide bridges.

The importance of disulfide bonds as a means for maintaining the native state integrity of extracellular proteins is widely acknowledged. Nevertheless, the mechanism by which these cross-links thermodynamically favor the folded tertiary structure remains a topic of considerable interest (Betz, 1993). It was proposed initially (Flory, 1956; Poland & Scheraga, 1965; Schellman, 1978) that disulfides exert their stabilizing effect by restricting the conformational freedom of the unfolded state, thereby decreasing the entropic barrier (ΔS_U) to protein folding. In this model (designated as the chain entropy model), the increase in stability attributed to disulfide formation is proportional to the logarithm of the loop size formed (usually expressed as the number of amino acid residues, *n*, between the two linked cysteines) (Pace et al., 1988). According to the chain entropy model, the largest gains in stabilization are for disulfide links that produce loops of moderate size (e.g., 3.0 kcal mol^{-1} for $n = 15$); stabilization increases only modestly for larger loops (cf. 3.6 kcal mol^{-1} for $n = 30$ and 4.7 kcal mol^{-1} for $n =$

† This work was supported by NIH Grant GM35976. NMR spectroscopy was carried out at the National Magnetic Resonance Facility at Madison which is funded by NIH Grant RR02301; equipment in the facility was purchased with funds from the University of Wisconsin, the NSF Biological Instrumentation Program (Grant DMB-8415048), the National Biomedical Research Technology Program (Grant RR02301), the NIH Shared Instrumentation Program (Grant RR02781), and the U.S. Department of Agriculture. A.P.H. was a trainee supported by an NIH Molecular Biophysics Training Grant (GM08293).

* To whom correspondence should be addressed.

‡ Present address, National Institute of Dental Research, 30 Convent Drive, Building 30, Room 132, Bethesda, MD 20892.

⊗ Abstract published in *Advance ACS Abstracts,* July 15, 1996.

[1] Abbreviations: ΔG_U, free energy change that accompanies protein unfolding; ΔH_U, enthalpy change that accompanies protein unfolding; ΔS_U, entropy change that accompanies protein unfolding; DTT, dithiothreitol; DMSO, dimethyl sulfoxide; HMQC-NOE, heteronuclear multiple quantum shift correlation experiment with a combined NOE relay period; HSMQC, heteronuclear single- and multiple-quantum shift correlation; IPTG, isopropyl β-D-thiogalactopyranoside; LB, Luria-Bertani bacterial growth medium; NMR, nuclear magnetic resonance; NOE, nuclear Overhauser effect; ppm, parts per million; PNPdTp, thymidine 3′-phosphate 5′-(*p*-nitrophenyl phosphate); PNP, *p*-nitrophenyl phosphate; pH*, pH value of ^2H_2O solutions uncorrected for the deuterium isotope effect; SDS−PAGE, sodium dodecyl sulfate−polyacrylamide gel electrophoresis; WT, recombinant protein produced in *Escherichia coli* whose sequence is identical to that of nuclease A isolated from the Foggi strain of *Staphylococcus aureus* [Tanuichi et al. (1967), as revised by Shortle (1983)]; H124L, recombinant protein produced in *E. coli* whose sequence is identical to that of nuclease A isolated from the V8 strain of *S. aureus* [Tanuichi et al. (1967), as revised by Shortle (1983)]. H124L differs from WT by the presence of leucine (rather than histidine) at position 124.

S0006-2960(96)00309-1 CCC: $12.00

100). Nature tends to use fairly short loop sizes (average of $n = 15$; Thornton, 1981).

The chain entropy model has been generally accepted, yet a number of recent studies [Matsumura et al., 1989; Doig & Williams, 1991; Tidor & Karplus, 1993; as reviewed by Betz (1993)] suggest that additional effects on both the folded and unfolded states are present. Chief among these are folded state enthalpic effects, which arise from local disruption of tightly packed protein structures; such effects have been observed experimentally in mutants of T4 lysozyme (Matsumura et al., 1989), subtilisin BPN′ (Mitchison & Wells, 1989), and barnase (Clarke & Fersht, 1993), as well as in a chemically modified form of hen egg white lysozyme (Cooper et al., 1992). Other proposed disulfide-induced folded state effects include entropic destabilization and a favorable hydrophobic effect. The former, which is thought to be mediated by conformational restriction of otherwise flexible portions of folded protein structures (Kuroki et al., 1992), has been supported by normal mode analysis of three BPTI variants lacking single disulfides (Tidor & Karplus, 1993). The latter effect was proposed on the basis of data for the transfer of model compounds from water to cyclohexane (Saunders et al., 1993) which indicated that the burial of a disulfide bond in a hydrophobic core is favored over the burial of two cysteine residues by 0.4 kcal mol^{-1}.

Alternative unfolded state effects also have been proposed. Doig and Williams (1991) suggested that disulfides both diminish the exposure of hydrophobic residues to solvent and interfere with favorable hydrogen bonding networks in the unfolded state. In direct opposition to the chain entropy model, this model predicts that the mechanism by which disulfides enhance stability is primarily enthalpic.

The primary goal of the study reported here has been to investigate and quantify folded state effects that accompany formation of engineered disulfides in the protein staphylococcal nuclease (nuclease). Naturally occurring forms of nuclease consist of a single polypeptide chain of 149 amino acids with no cysteine and no cross-links. The structure of nuclease has been characterized by both X-ray crystallography (Cotton & Hazen, 1979; Loll & Lattman, 1989; Hynes & Fox, 1991; Truckses et al., 1996) and multinuclear NMR spectroscopy (Torchia et al., 1989a,b; Wang et al., 1990a−c). Nuclease has also served as a model system for sequence effects on the structures of both the folded (Sondek & Shortle, 1990; Alexandrescu et al., 1990) and unfolded (Shortle et al., 1990; Green et al., 1992) states. Of the proteins that have been studied most extensively, nuclease is one of the least stable; its ΔG for global unfolding is only 5−6 kcal mol^{-1} at room temperature and neutral pH.

One interesting feature of nuclease is that its folded state exhibits structural heterogeneities that arise from *cis/trans* isomerizations about the Lys^{116}−Pro^{117} (Evans et al., 1987; Alexandrescu, 1988) and His^{46}−Pro^{47} (Loh et al., 1991) peptide bonds. These conformational states interconvert slowly on the time scale of the chemical shift perturbations that they engender. For example, the $^1H^{\epsilon 1}$ NMR signals from His^8, His^{124}, and His^{121} from protein molecules with a *cis* Lys^{116}−Pro^{117} peptide bond are distinct from those from molecules with a *trans* peptide bond at this position; similarly, the $^1H^{\epsilon 1}$ signal from His^{46} from protein molecules with a *cis* His^{46}−Pro^{47} peptide bond are distinct from those from molecules with a *trans* peptide bond at this position. The relative intensities of the pairs of peaks from individual histidines can be used as an assay of the relative populations of the conformational substates to which these peaks are sensitive. Although in the X-ray structures of nuclease (Cotton & Hazen, 1979; Loll & Lattman, 1989; Hynes & Fox, 1991; Truckses et al., 1996) the His^{46}−Pro^{47} peptide bond is modeled as *trans* and the Lys^{116}−Pro^{117} peptide bond is modeled as *cis*, in solution, nuclease has a 20:80 *cis*:*trans* ratio at His^{46}−Pro^{47} (Loh et al., 1991) and a 90:10 *cis*:*trans* ratio at Lys^{116}−Pro^{117} (Evans et al., 1987, 1989; Alexandrescu, 1988; Hinck et al., 1993).

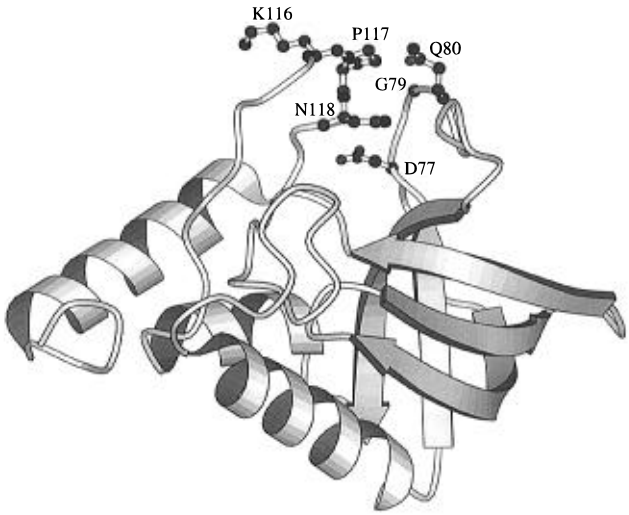

FIGURE 1: Ribbon diagram, based on the X-ray structure of wild-type nuclease (WT) (Loll & Lattman, 1989), depicting the locations of the residues that were substituted by cysteine in the investigation reported here.

Our motivation for the current work follows from experimental results first reported by Evans et al. (1989) and Alexandrescu et al. (1990) and more recently by Hinck (1993), Hinck et al. (1993), Loh (1993), and Hodel et al. (1993, 1994, 1995) which suggest that specific favorable interactions localized near the N- and C-terminal ends of the type VI$_a$ β turn containing *cis* Pro^{117} are responsible for destabilization of the intrinsically favorable *trans* Lys^{116}−Pro^{117} peptide bond (Raleigh et al., 1992; Hodel, 1993). Thus, our hypothesis was that disulfide bonds engineered to span the extended turn containing Gly^{79} and the type VI$_a$ reverse turn containing Pro^{117} should be coupled to a configurational preference for Pro^{117}. Disulfides that lead to enhanced loop anchorage or that reinforce backbone torsion angles characteristic of the *cis* geometry should increase the proportion of the *cis* form, whereas those that diminish loop anchorage or interfere with the set of backbone torsion angles consistent with the *cis* isoform are predicted to result in an increase of the *trans* form in the folded protein. To test this model, four different nuclease mutants containing single-residue substitutions to cysteine on each of the two loops were constructed: H124L$^{C77-C118}$, H124L$^{C79-C118}$, H124L$^{C80-C116}$, and G79S+H124L$^{C80-C116}$.[1] The positions of the substituted residues are indicated in Figure 1.

The stabilities of the engineered proteins were analyzed by a four-state unfolding model, using data obtained for the free energies for global unfolding, both in the presence and in the absence of disulfide cross-links along with folded state reduction potentials. The results suggest that varying levels of folded state strain are present. Additional data obtained by monitoring the configurational state of the Lys^{116}−Pro^{117}

peptide by NMR revealed that the level of strain present in each of the mutants, as determined by equilibrium stability measurements, is correlated with the perturbation free energy, $\Delta G_{c/t}$, the free energy change which accompanies *cis/trans* isomerization of the Lys^{116}−Pro^{117} peptide bond upon disulfide formation.

EXPERIMENTAL PROCEDURES

Synthesis of Isotopically Labeled Amino Acids. [$^{13}C^{\alpha}$, $^{13}C^{\alpha\prime}$]-D,L-Cystine (0.18 g) was prepared in an overall yield of 22% by the procedure described by Atkinson et al. (1953) (Figures 1 and 2, in the supporting information), with [2-^{13}C] diethyl acetamidomalonate (Hinck et al., 1993) being used in place of unlabeled diethyl acetamidomalonate. ^{1}H NMR (^2H_2O): δ 1.62 (m, H-3,3′, 4H), 2.72 (dt, H-2, $^1J_{CH}$ = 149 Hz, 2H). ^{13}C NMR (^2H_2O): δ 51.8. [$^{13}C^{\alpha}$]-D,L-Proline and [$^{13}C^{\alpha}$]-D,L-lysine were synthesized by procedures described previously (Hinck et al., 1993).

Plasmids Used for Overproducing the Nuclease Mutants. Plasmid pTSN2cc encodes nuclease H124L, which is identical to the nuclease A isolated from the V8 strain of *Staphylococcus aureus.* The D77C, G79C, Q80C, K116C, N118C, and G79S+Q80C single and double mutants of the pTSN2cc plasmid were generated by one and two rounds of mutagenesis, respectively. Owing to the unique location of a *Hin*dIII restriction site near the codon for amino acid 101 in the nuclease gene, simultaneous restriction digests with *Hin*dIII and *Pst*I followed by recombination of the appropriate DNA fragments permitted the construction of each of the four double-cysteine mutant genes. Each was confirmed by double-stranded dideoxy sequencing of the recombinant overproducing plasmids.

Protein Expression and Purification. Each of the recombinant nucleases was produced by using the T7 expression system with *Escherichia coli* strain BL21(DE3) and plasmid pLysS. Cells were cultured in LB medium supplemented with 50 μg/mL ampicillin and 34 μg/mL chloramphenicol, and recombinant nuclease was purified by a combination of A-25 DEAE Sephadex and C-25 CM-Sephadex column chromatography as described previously (Royer et al., 1993). The final eluate was found by nonreducing SDS−PAGE to contain two species, which had apparent molecular masses of approximately 17 and 34 kDa; analysis of the same samples by reducing SDS−PAGE revealed a single band of 17 kDa. The 34 kDa band was presumed to be dimers linked by interchain disulfide bridges. Monomeric nuclease was isolated by concentrating the sample to 20 mg/mL by ultrafiltration (PM-10 disc membrane, Amicon, Beverly, MA) and by passing the material over a 2.5 × 75 cm column of high-resolution Sephacryl S-100 HR at a flow rate of 0.5 mL/min. The peak corresponding to monomeric nuclease was pooled and concentrated to 20 mg/mL by ultrafiltration, and the procedure was repeated. The final product was pooled, dialyzed into pure water (Royer et al., 1993), and lyophilized. Analysis by nonreducing SDS−PAGE revealed a single 17 kDa band. Subsequent examination of samples stored at room temperature for periods of up to 1 month revealed no changes in sample composition.

Determination of Free Thiols. The free thiol content of a purified, monomeric sample of each of the nuclease mutants was determined by reaction with DTNB (Jocelyn, 1987). In this assay, free thiols are modified with stoichiometric production of MNB, which is assayed spectrophotometrically; the following extinction coefficient for MNB was employed, $\epsilon_{412} = 1.415 \times 10^4$ M^{-1} cm^{-1} (Jocelyn, 1987). Protein concentrations were determined spectrophotometrically by measuring the absorbance at 280 nm; the extinction coefficient used for nuclease was $\epsilon_{280} = 1.83 \times 10^4$ M^{-1} cm^{-1} (Cuatrecasas, 1967).

Enzyme Assays. Nuclease samples were assayed against the mononucleotide substrate, thymidine 3′-phosphate 5′-(*p*-nitrophenyl phosphate) (PNPdTP), as described by Grissom and Markley (1989). All assays were carried out at 28 °C in 0.1 M CHES (pH 9.5) with 0.1 M $CaCl_2$ and 0.2 M KCl. Initial velocities for formation of the product, *p*-nitrophenyl phosphate (PNP), were monitored at 330 nm on a Hewlett-Packard 8452 diode array spectrophotometer. The extinction coefficient of PNP was assumed to be 9.4×10^3 M^{-1} cm^{-1} (Grissom & Markley, 1989). The concentrations of wild-type and mutant nucleases were determined spectrophotometrically as described above. K_m and k_{cat} values were calculated by fitting the initial velocities and substrate concentrations to

$$v = \frac{V_{max}S}{K_m + S} \quad (1)$$

with the ENZFITTER package (Biosoft, Cambridge, England).

Use of NMR Spectroscopy To Monitor Protein Unfolding at Elevated Temperatures. Protein samples were prepared in ^2H_2O as described by Alexandrescu (1990). The pH* values of samples used for thermal unfolding studies were between 5.1 and 5.3, and the protein concentrations were between 1.0 and 2.0 mM. Reduced nuclease samples were prepared by adding a 30-fold molar excess of solid DTT directly to the NMR sample tube. Reduction, which was monitored over time by following the histidine $^1H^{\epsilon 1}$ peaks corresponding to the oxidized and reduced forms, was found to be complete within about 5 min following the addition of DTT. Thermal unfolding data were collected on a Bruker AM 500 spectrometer operating at 499.84 MHz which was equipped with a variable-temperature 5 mm ^{1}H probe. The thermocouple in the probe was calibrated over the range of temperatures of the unfolding experiments (300−340 K) by measuring the separation of two resonances in a sample of 80% ethylene glycol/20% DMSO-d_6 (Bruker user's manual). Spectra were collected at 1 °C temperature increments on either side of the thermal unfolding transition in an interleaved fashion. In all cases, the transitions were found to be reversible.

The areas of the histidine $^1H^{\epsilon 1}$ peaks in spectra obtained at each temperature were fitted to Lorentzian line shapes as described previously (Royer et al., 1993). Histidine resonances arising from the folded *cis* and *trans* forms were fitted separately; resonances arising from the individual histidines in the unfolded state could not be resolved and were fitted to (usually three) overlapping peaks. The two-state equilibrium constant for unfolding,

$$K_U^{thermal} = (U_{cis} + U_{trans})/(F_{cis} + F_{trans}) \quad (2)$$

was determined by summing the areas of the best-fitted unfolded (U) and folded (F) resonances and by taking the quotient, U/F (eq 2). Thermodynamic parameters for revers-

ible unfolding of the protein were obtained from the van't Hoff formalism:

$$\partial[\ln(K_U^{thermal})]/\partial\left(\frac{1}{T}\right) = -\Delta H_U^{thermal}/R \quad (3)$$

$\Delta H_U^{thermal}$ and $\Delta S_U^{thermal}$ and the associated errors for the unfolding were calculated from linear fittings of $\ln(K_U^{thermal})$ versus $1/T$. The equilibrium constant for the *cis/trans* interconversion at $Xxx^{116}-Pro^{117}$ was calculated from F_{cis}/F_{trans} and is designated $K_{c/t}$.

$$F_{trans} \rightleftharpoons F_{cis} \quad (4)$$

Assignment of NMR Signals to Individual Configurational States of the $Xxx^{116}-Pro^{117}$ Peptide Bond by Isotope-Edited NMR Spectroscopy of Samples Labeled Selectively with ^{13}C. The T7 overexpressing plasmids encoding $H124L^{C80-C116}$, $G79S+H124L^{C80-C116}$, $H124L^{C79-C118}$, and $H124L^{C77-C118}$ were first cotransformed along with plasmid pLysS (Novagen, Madison, WI) into *E. coli* strain WGTK1 (*putPA proC lysA)*, which contains the IPTG inducible gene for T7 RNA polymerase (Hinck et al., 1993). Nucleases $H124L^{C80-C116}$ and $G79S+H124L^{C80-C116}$ were labeled selectively with [$^{13}C^{\alpha}$]Cys and [$^{13}C^{\alpha}$]Pro by including [$^{13}C^{\alpha}$, $^{13}C^{\alpha\prime}$]-D,L-cystine and [$^{13}C^{\alpha}$]-D,L-proline at a level of 50 mg/L each in a defined minimal medium as described previously (Hinck et al., 1993). Nucleases $H124L^{C79-C118}$ and $H124L^{C77-C118}$ were labeled selectively with [$^{13}C^{\alpha}$]Lys and [$^{13}C^{\alpha}$]Pro by an analogous procedure by including [$^{13}C^{\alpha}$]-D,L-proline (50 mg/L) and [$^{13}C^{\alpha}$]-D,L-lysine (100 mg/L). The selectively labeled nucleases were isolated and purified by the procedure employed for unlabeled samples. The four labeled nuclease samples were then analyzed individually in their oxidized and reduced states by the HSMQC and HMQC-NOE experiments as described previously (Hinck et al., 1993). Reduced samples were prepared by adding a 30-fold molar excess of solid DTT and were analyzed in a manner otherwise identical to that of the oxidized samples.

Use of Fluorescence Spectroscopy To Monitor the Folding/Unfolding Equilibrium in the Presence of Guanidinium Chloride. The intrinsic tryptophan fluorescence of the protein at 294.5 K and pH 5.50 was measured as a function of guanidinium chloride (GdmCl) concentration. In practice, small aliquots of a 6.00 M GdmCl solution were added to 2.00 mL of a 75 μg/mL protein solution contained in 10 mM Bis-Tris (pH 5.50) as described by Shortle (1986). Titrations of nucleases in the reduced state were carried out by first incubating the 75 μg/mL protein solution in the presence of 10 mM DTT for 10 h at pH 8.0 and then by adjusting the pH to 5.50 with small aliquots of dilute HCl before stepwise addition of a GdmCl solution as above. An ISS Koala spectrofluorimeter (ISS, Champaign, IL), with excitation from a tungsten lamp at 295 nm (2 nm band width) and detection at 325 nm (2 nm band width), was used for the fluorescence intensity measurements. Eighteen to 30 points were collected for each mutant. Complete reversibility of the unfolding reactions for the oxidized and reduced forms of each protein was demonstrated by recovery of 98−102% of the folded fluorescence intensity upon dilution of the sample. Raw fluorescence intensities corrected for sample dilution were fitted in a nonlinear fashion to eq 5:

$$\ln(K_{app}) = \ln(K_U^{GdmCl}) + m[\text{GdmCl}] \quad (5)$$

where K_{app} is defined as

$$K_{app} = (I_F - I)/(I - I_U) \quad (6)$$

where I is the observed fluorescence intensity, I_F is the limiting fluorescence intensity for the folded protein, I_U is the limiting fluorescence intensity for the unfolded protein, and ΔG_U^{GdmCl} is the equilibrium constant for unfolding in the absence of denaturant (Pace, 1975; Shortle, 1986). Unfolding reactions of the oxidized and reduced forms of each mutant were carried out in triplicate.

Dithiothreitol Reduction and HPLC Analysis. The equilibrium constant for the reduction of each mutant by DTT

$$DTT_{SH}^{SH} + \text{protein}_{S-S} \rightleftharpoons DTT_{S-S} + \text{protein}_{SH}^{SH} \quad (7)$$

was measured by incubating 10.6 μg of the protein in 200 μL of N_2-purged 10 mM potassium phosphate buffer (pH 8.00) containing varying ratios of DTT and *trans*-4,5-dihydroxy-1,2-dithiane (oxidized DTT, Sigma, St. Louis, MO) for 4 h at room temperature under an atmosphere of N_2. The ratios and concentrations of DTT_{SH}^{SH} to DTT_{S-S} utilized were 0.000 33 (0.050 mM:150 mM), 0.000 50 (0.075 mM:150 mM), 0.000 75 (0.113 mM:150 mM), 0.0010 (0.15 mM:150 mM), 0.0015 (0.225 mM:150 mM), 0.0020 (0.300 mM:150 mM), 0.0030 (0.45 mM:150 mM), 0.0050 (0.75 mM:150 mM), 0.0075 (1.13 mM:150 mM), 0.010 (1.50 mM:150 mM), and 0.020 (1.5 mM:75 mM), respectively. The reaction was quenched by the addition of 100 μL of 0.2 M acetic acid, and the samples were analyzed by injecting 50 μL of each redox mixture onto a 4.6 mm × 150 mm silica-based C4 reverse phase HPLC column (Vydac, Hesperia, CA) equilibrated in 80:20 H_2O (0.1% TFA)/acetonitrile (0.1% TFA). Separation of the oxidized and reduced forms was achieved by a linear gradient ranging from 60:40 to 50:50 H_2O/CH_3CN over a period of 8 min at a flow rate of 1 mL/min. The data were exported from the HPLC system in the ASCII format and were analyzed by fitting the peaks for the oxidized and reduced forms to overlapping distorted exponential line shapes with linear baseline corrections (PEAKFIT, Jandel Scientific, San Rafael, CA). Equilibrium constants were calculated from the equation

$$K_{Red}^{F} = [DTT_{S-S}][\text{protein}_{SH}^{SH}]/[DTT_{SH}^{SH}][\text{protein}_{S-S}] \quad (8)$$

by multiplying the peak ratios for the reduced to oxidized protein by the ratio of DTT_{S-S} and DTT_{SH}^{SH} added to the redox buffer. The effect of protein on this ratio should be negligible since the minimum ratios of DTT_{SH}^{SH}:protein and DTT_{S-S}:protein employed were 16 and 2.4×10^4, respectively. Statistical estimates of K_{Red}^{F} were determined by calculating K_{Red}^{F} for $0.2 \leq \text{protein}_{SH}^{SH}/\text{protein}_{S-S} \leq 4.0$.

RESULTS

Sample Preparation and Enzymatic Activity. Nonreducing SDS−PAGE analysis of the four double-cysteine mutants of nuclease as isolated from *E. coli* revealed a mixture of monomeric and dimeric forms. These forms were separated by gel filtration column chromatography, and the pure monomeric species was obtained in high yield. Disulfide

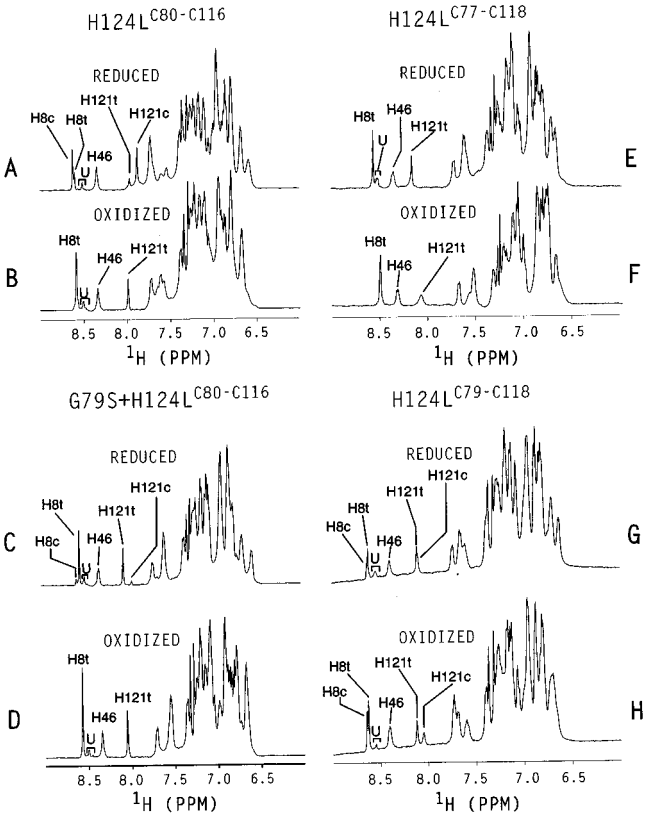

FIGURE 2: Aromatic region of one-dimensional, 500 MHz, ^{1}H NMR spectra of nuclease variants: (A and B) H124L$^{C80-C116}$, (C and D) G79S+H124L$^{C80-C116}$, (E and F) H124L$^{C77-C118}$, and (G and H) H124L$^{C79-C118}$ recorded in ^2H_2O, at pH* 5.50 and 312 K. The lower spectra (B, D, F, and H) are of the oxidized proteins, whereas the upper spectra (A, C, E, G) were recorded under conditions (30-fold molar excess of DTT) where the engineered disulfides are reduced quantitatively. Individual histidine $^1H^{\epsilon 1}$ resonances are labeled with the residue number and the conformational form to which they have been assigned (t, *trans*; c, *cis*). U indicates $^1H^{\epsilon 1}$ signals arising from unfolded protein.

pairing was assessed by investigating the reaction of each mutant with DTNB (Joceyln, 1987). The results (supporting information, Table 1) confirmed the presence of the two cysteine residues introduced by mutagenesis and proved that the disulfide bonds were correctly and completely formed. In addition, each of the mutants maintained hydrolytic activity toward 5′-phosphates as demonstrated by their ability to cleave 3′-phosphate 5′-(*p*-nitrophenyl phosphate) into *p*-nitrophenyl phosphate and thymidine 3′-phosphate (supporting information, Table 2). The catalytic efficiency (k_{cat}/K_m) of the mutants, however, was diminished by between 5- and 400-fold relative to that of the wild-type. The decrease in k_{cat}/K_m is due largely to a reduction in k_{cat} and appears to be affected by both the amino acid substitutions and disulfide bond formation.

Configurational Analysis. Figure 2 shows the aromatic and aliphatic portions of the one-dimensional ^{1}H NMR spectra of each of the four disulfide mutants under reducing and nonreducing conditions. Spectra of the oxidized forms of H124L$^{C80-C116}$, G79S+H124L$^{C80-C116}$, and H124L$^{C77-C118}$ revealed no detectable splittings in the $^1H^{\epsilon 1}$ signals from His^8 and His^{121}. By contrast, the spectrum of oxidized H124L$^{C79-C118}$ showed a clear splitting of His^8 and His^{121} into major and minor components. Because the chemical shifts and relative intensities of the major and minor components were similar to those reported previously for the G79S mutant (Hinck et al., 1993), these were presumed to correspond to the signals arising from the *trans* and *cis* folded forms, respectively.

Table 1: Experimental Values for the Equilibrium Constant ($K_{c/t}$) and Derived Thermodynamic Quantities for the Isomerization Reaction ($F_{trans} \rightleftharpoons F_{cis}$) at the Xxx^{116}−Pro^{117} Peptide Bond in Nuclease H124L and the Oxidized and Reduced Forms of Its Engineered Disulfide Mutants

protein variant	$K_{c/t}$[a]	$\Delta G_{c/t}$[b] (kcal mol^{-1})	$\Delta\Delta G_{c/t}$[c] (kcal mol^{-1})
H124L	14.3 ± 4.1	−1.7 ± 0.2	
H124L$^{C80-C116}$ (oxidized)	<0.01[d]	>2.9	
H124L$^{C80-C116}$ (reduced)	2.8 ± 1.2	-0.65 ± 0.26	<−3.5
G79S+H124L$^{C80-C116}$ (oxidized)	<0.01[d]	>2.9	
G79S+H124L$^{C80-C116}$ (reduced)	0.16 ± 0.01	1.2 ± 0.1	<−1.7
H124L$^{C79-C118}$ (oxidized)	0.77 ± 0.06	0.17 ± 0.05	
H124L$^{C79-C118}$ (reduced)	0.34 ± 0.01	0.67 ± 0.02	+0.50
H124L$^{C77-C118}$ (oxidized)	< 0.01[d]	> 2.9	
H124L$^{C77-C118}$ (reduced)	< 0.01[d]	> 2.9	0.0

[a] Equilibrium constant ($K_{c/t}$) for the isomerization reaction ($F_{trans} \rightleftharpoons F_{cis}$) at the Xxx^{116}−Pro^{117} peptide bond at 318K; $K_{c/t} = [F_{cis}]/[F_{trans}]$. [b] $\Delta G_{c/t} = -RT \ln(K_{c/t})$. [c] $\Delta\Delta G_{c/t} = (\Delta G_{c/t}$ oxidized) − ($\Delta G_{c/t}$ reduced). [d] This represents the lower limit of detection of the $^1H^{\epsilon 1}$ resonances in one-dimensional ^{1}H NMR spectra.

Upon reduction, splittings were evident in spectra of H124L$^{C80-C116}$ and G79S+H124L$^{C80-C116}$. The *cis/trans* equilibria paralleled those found in the respective parent proteins, H124L (Alexandrescu et al., 1990) and G79S+H124L (Hinck et al., 1993), although the equilibria were shifted somewhat farther in favor of the *trans* forms (Table 1). NMR spectra of reduced H124L$^{C79-C118}$ revealed *cis*/*trans* heterogeneity, with the equilibrium shifted by a factor of approximately 2 in favor of the *trans* form (Table 1). The $^1H^{\epsilon 1}$ signals of H124L$^{C77-C118}$ remained unsplit.

For those species that displayed no detectable histidine $^1H^{\epsilon 1}$ splittings (nonreduced forms of H124L$^{C80-C116}$ and G79S+H124L$^{C80-C116}$ and both oxidation states of H124L$^{C77-C118}$), the position of the 116−117 *cis*/*trans* equilibrium was analyzed by isotope-edited NMR spectroscopy of samples labeled selectively with ^{13}C at the Xxx and Pro residues. This method, which has been previously applied to H124L and several nuclease mutants (Hinck et al., 1993), provides a direct means of assessing the predominant configuration of the peptide bond spanning the labeled residues.

In the HSMQC spectrum of oxidized H124L$^{C80-C116}$ labeled selectively with [$^{13}C^{\alpha}$]Cys and [$^{13}C^{\alpha}$]Pro (supporting information, Figure 3A), five peaks, grouped near 62 ppm in the ^{13}C dimension, were assigned tentatively to proline $^1H^{\alpha}-^{13}C^{\alpha}$ resonances. Of the three additional $^1H^{\alpha}-^{13}C^{\alpha}$ peaks, the two having ^{13}C shifts of approximately 53 ppm were assigned tentatively to Cys $^1H^{\alpha}-^{13}C^{\alpha}$ resonances. The remaining peak, which was close to the group of proline resonances, but displaced somewhat upfield in both the ^{13}C and ^{1}H dimensions, was assigned tentatively as the sixth proline. The HMQC-NOE spectrum of the same sample (supporting information, Figure 3B) showed no intraresidue NOE cross-peaks between any of the Cys and Pro $^1H^{\alpha}-^{13}C^{\alpha}$ direct correlation cross peaks. Such NOE cross-peaks are diagnostic for *cis* Xxx−Pro peptide bonds (Hinck et al., 1993; Wüthrich et al., 1986). Thus, it was concluded that the configuration of the Cys^{116}−Pro^{117} peptide bond in the oxidized form of H124L$^{C80-C116}$ is predominantly *trans*.

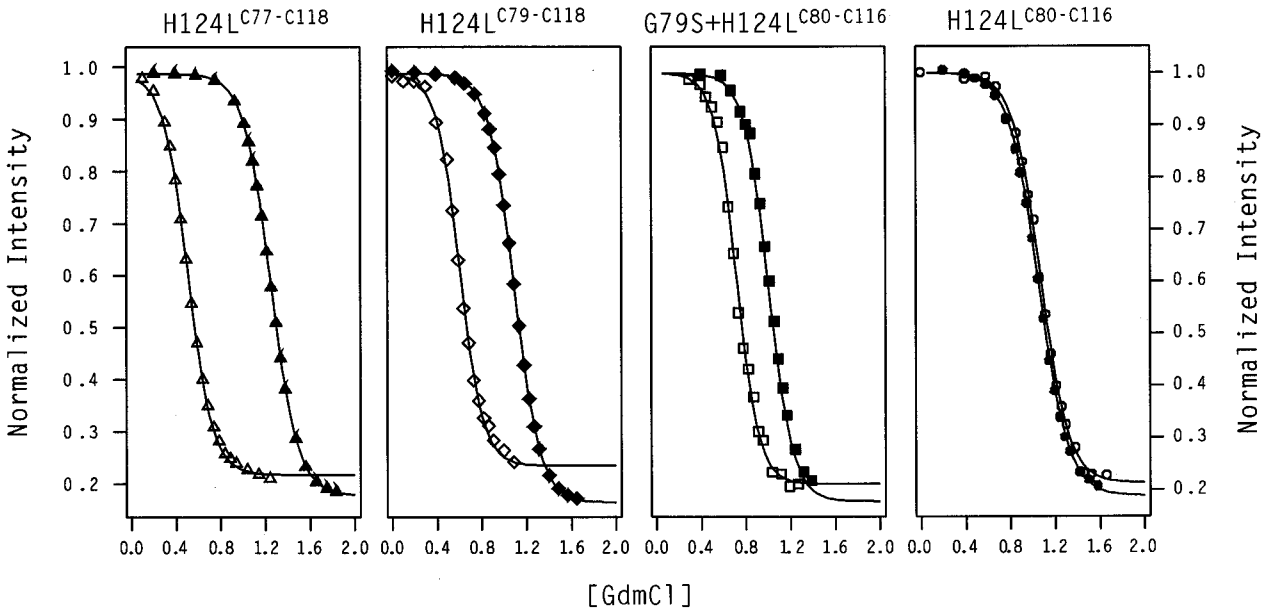

FIGURE 3: Representative guanidinium chloride unfolding curves for the four disulfide mutants of nuclease in their oxidized and reduced states. Intrinsic fluorescence emission intensities at 325 nm were recorded, at a temperature of 294.5 K, as a function of increasing concentration of GdmCl. Filled symbols denote data collected for samples under oxidizing conditions, whereas open symbols correspond to data collected in the presence of 10 mM DTT.

To validate the experimental strategy, this sample was reduced and analyzed by the same repertoire of experiments. In the reduced state, the one-dimensional NMR results presented above indicated that the Cys^{116}−Pro^{117} peptide bond is predominantly *cis*. This prediction was confirmed by HSMQC and HMQC-NOE spectra of the reduced protein. In the HSMQC spectrum (supporting information, Figure 3C), six cross-peaks were found grouped near 62 ppm (^{13}C dimension). These resonances, which correspond closely to $^{1}H^{\alpha}-^{13}C^{\alpha}$ correlations reported in the spectrum of WT (Torchia et al., 1989), were assigned to the corresponding residues of the mutant. Of the three additional cross-peaks, one had the same $^{1}H-^{13}C$ chemical shift as the cross-peak tentatively assigned to the sixth proline in the nonreduced spectrum, which suggests it arises from incomplete reduction of this sample or partial oxidation of DTT during the course of the experiment. The remaining two cross-peaks were assigned to cysteinyl $^{1}H^{\alpha}-^{13}C^{\alpha}$ resonances. In the HMQC-NOE spectrum (supporting information, Figure 3D), one of the cysteine peaks (Cys^{a}) showed a strong NOE cross-peak to $^{1}H^{\alpha}-^{13}C^{\alpha}$ of Pro^{117}. Similarly, the cross-peak assigned to Pro^{117} showed a strong cross-peak to Cys^{a}. Thus, these data, in conjunction with the heterogeneity observed for the histidine resonances, are consistent with a predominantly *cis* Cys^{116}−Pro^{117} peptide bond in the reduced form of H124L$^{C80-C116}$.

The configuration of Pro^{117} in the oxidized and reduced forms of G79S+H124L$^{C80-C116}$ and H124L$^{C77-C118}$ also has been investigated by selective isotope labeling. For G79S+H124L$^{C80-C116}$, [$^{13}C^{\alpha}$]Cys and [$^{13}C^{\alpha}$]Pro were incorporated, whereas for H124L$^{C77-C118}$, [$^{13}C^{\alpha}$]Lys and [$^{13}C^{\alpha}$]-Pro were utilized. A comparison of the HSMQC and HMQC-NOE spectra for these mutants under both nonreducing and reducing conditions (data not shown), however, revealed no detectable NOEs between either Cys $^{1}H^{\alpha}$ and Pro $^{1}H^{\alpha}$ or Lys $^{1}H^{\alpha}$ and Pro $^{1}H^{\alpha}$. Therefore, it was concluded that the peptide bond configuration of Pro^{117} is predominantly *trans* for both mutants in both oxidation states. Additional evidence consistent with these conclusions is provided by splittings of the histidine peaks in the reduced form of G79S+H124L$^{C80-C116}$, which indicate that the Pro^{117} peptide bond is predominantly *trans*, and by previous results obtained with the D77A mutant (Hinck, 1993; Hinck et al., 1993), which indicate that mutants of Asp^{77} strongly perturb the *cis/trans* equilibrium in favor of the *trans* form.

The effects of oxidation and reduction of the engineered disulfide in each of the four protein variants on local structure as revealed by changes in the configurational preference at the Xxx^{116}−Pro^{117} peptide bond are summarized in Table 1. These data indicate that disulfide bond formation significantly perturbs the equilibrium for three of the mutants. In H124L$^{C79-C118}$, the effect of the engineered disulfide bond is to shift the *cis*/*trans* equilibrium in favor of the *cis* form by a factor of 2, whereas in H124L$^{C80-C116}$ and G79S+H124L$^{C80-C116}$, disulfide formation favors the *trans* form. Formation of the disulfide bridge in H124L$^{C77-C118}$ has little effect on the configuration of the Lys^{116}−Pro^{117} peptide bond, which remains predominantly *trans* in both oxidation states.

Protein Stabilities. The consequences of the engineered disulfide bonds on stability were evaluated by two independent methods. In the first, the stability to unfolding of the oxidized and reduced forms of the protein were determined by monitoring the intrinsic fluorescence of Trp^{140} as a function of guanidinium chloride (GdmCl) concentration. Each mutant, under both sets of redox conditions, displayed the characteristic loss of tryptophan fluorescence that accompanies unfolding of staphylococcal nuclease (Figure 3). The data were fitted to a two-state unfolding model in a nonlinear fashion to yield the free energy of unfolding in the absence of denaturant, ΔG_U^{GdmCl}, and the *m* value, the rate of change in $\ln(K_U^{GdmCl})$ as a function of the concentration of GdmCl (Table 2). None of the mutants was more stable than H124L, although the concentration of GdmCl at the midpoint of the unfolding transition, C_m, was lower for H124L than for the oxidized forms of H124L$^{C79-C118}$ and H124L$^{C77-C118}$. It was also found that the *m* values for all

Table 2: Parameters Describing the Guanidinium Chloride-Induced Unfolding of Nuclease H124L and the Oxidized and Reduced Forms of Its Engineered Disulfide Mutants[a]

protein variant	C_m (M)	m (M^{-1})	m_{rel}[b]	ΔG_U^{GdmCl} (kcal mol^{-1})	$\Delta\Delta G_U^{GdmCl}$ (kcal mol^{-1})[c]
H124L	1.05 ± 0.03	10.65 ± 0.27	1.00	5.98 ± 0.22	
H124L$^{C80-C116}$ (oxidized)	1.05 ± 0.02	8.08 ± 0.41	0.76	4.98 ± 0.26	
H124L$^{C80-C116}$ (reduced)	1.06 ± 0.01	8.65 ± 0.51	0.81	5.39 ± 0.29	−0.41
G79S+H124L$^{C80-C116}$ (oxidized)	1.00 ± 0.01	9.36 ± 0.23	0.88	5.50 ± 0.14	
G79S+H124L$^{C80-C116}$ (reduced)	0.73 ± 0.01	10.45 ± 0.46	0.99	4.49 ± 0.26	1.01
H124L$^{C79-C118}$ (oxidized)	1.08 ± 0.01	8.76 ± 0.08	0.82	5.55 ± 0.01	
H124L$^{C79-C118}$ (reduced)	0.60 ± 0.01	9.31 ± 0.68	0.87	3.27 ± 0.28	2.28
H124L$^{C77-C118}$ (oxidized)	1.23 ± 0.02	8.25 ± 0.11	0.78	5.95 ± 0.14	
H124L$^{C77-C118}$ (reduced)	0.52 ± 0.02	9.04 ± 0.46	0.85	2.76 ± 0.25	3.19

[a] Samples were dissolved in 10 mM Bis-Tris buffer at pH 5.50 and $T = 294.5$ K. [b] Values are relative to the m value of H124L (10.65 M^{-1}). [c] $\Delta\Delta G_U^{GdmCl} = (\Delta G_U^{GdmCl}$ oxidized) − (ΔG_U^{GdmCl} reduced).

Table 3: Thermodynamic Parameters for Thermal Unfolding of Nuclease H124L and the Oxidized and Reduced Forms of Its Engineered Disulfide Mutants[a]

protein variant	$\Delta H_U^{thermal}$ (kcal mol^{-1})	$\Delta S_U^{thermal}$ (kcal mol^{-1} K^{-1})	T_m (K)	$\Delta G_U^{thermal}$ (kcal mol^{-1})[b]	$\Delta\Delta G_U^{thermal}$ (kcal mol^{-1})[c]
H124L	90.3 ± 2.1	0.27 ± 0.02	329.0 ± 0.9	4.39 ± 0.43	
H124L$^{C80-C116}$ (oxidized)	55.2 ± 2.4	0.17 ± 0.02	331.0 ± 1.9	3.00 ± 0.31	
H124L$^{C80-C116}$ (reduced)	52.8 ± 5.6	0.16 ± 0.02	324.2 ± 0.5	1.83 ± 0.41	1.15
G79S+H124L$^{C80-C116}$ (oxidized)	67.3 ± 4.5	0.21 ± 0.01	326.9 ± 3.1	2.85 ± 0.37	
G79S+H124L$^{C80-C116}$ (reduced)	33.1 ± 2.2	0.10 ± 0.01	316.1 ± 2.8	0.32 ± 0.08	2.53
H124L$^{C79-C118}$ (oxidized)	80.9 ± 2.9	0.24 ± 0.01	337.4 ± 1.7	5.85 ± 0.44	
H124L$^{C79-C118}$ (reduced)	69.0 ± 1.7	0.21 ± 0.01	322.0 ± 1.1	1.92 ± 0.34	3.93
H124L$^{C77-C118}$ (oxidized)	46.3 ± 1.7	0.14 ± 0.01	327.0 ± 1.8	1.98 ± 0.24	
H124L$^{C77-C118}$ (reduced)	37.6 ± 2.6	0.12 ± 0.01	303.0 ± 4.1	−1.24 ± 0.21	3.22

[a] Enthalpies, entropies, and melting temperatures are for the F ⇌ U unfolding transition in ^2H_2O at pH* 5.5. [b] Values are calculated from $\Delta G_U^{thermal} = \Delta H_U^{thermal} - T\Delta S_U^{thermal}$, $T = 313$ K. [c] $\Delta\Delta G_U^{thermal} = (\Delta G_U^{thermal}$ oxidized) − ($\Delta G_U^{thermal}$ reduced).

mutants, in both their oxidized and reduced states, are generally lower than that of H124L (Table 2). The *m* values for the reduced forms were generally greater than those of their oxidized counterparts. Among the mutants, considerable variation in ΔG_U^{GdmCl} accompanied disulfide formation; the oxidized form of H124L$^{C77-C118}$ was 3.19 kcal mol^{-1} more stable than its reduced form, whereas the oxidized form of H124L$^{C80-C116}$ was actually 0.41 kcal mol^{-1} less stable than its reduced form (Table 2).

The second method used to measure stability of the disulfide mutants was to follow the histidine $^1H^{\epsilon 1}$ resonances as a function of temperature. Linear portions of plots of ln($K_U^{thermal}$) versus 1/T (van't Hoff plots) for each of the mutants in their oxidized and reduced states are presented in Figure 4. Among the mutants studied at 40 °C, only H124L$^{C79-C118}$ in its oxidized form possessed a stability greater than that of H124L (Table 3). Enthalpy values followed a similar trend. $\Delta H_U^{thermal}$ for the disulfide form of H124L$^{C79-C118}$ was just 9.6 kcal mol^{-1} lower than $\Delta H_U^{thermal}$ for H124L, whereas $\Delta H_U^{thermal}$ values for the remainder of the mutants were considerably lower. As with the GdmCl data, considerable variation was found in the effects of disulfide formation on protein stability (Table 3). $\Delta G_U^{thermal}$ increased by 3.9 kcal mol^{-1} for H124L$^{C79-C118}$, by 3.2 kcal mol^{-1} for H124L$^{C77-C118}$, by 2.5 kcal mol^{-1} for G79S+H124L$^{C80-C116}$, and by 1.2 kcal mol^{-1} for H124L$^{C80-C116}$. These variations in $\Delta G_U^{thermal}$ were also reflected in large changes in midpoint unfolding temperatures (T_m). The change in midpoint unfolding accompanying disulfide formation, ΔT_m, was 24.6 °C for H124L$^{C77-C118}$, 15.0 °C for H124L$^{C79-C118}$, 10.8 °C for G79S+H124L$^{C80-C116}$, and 5.8 °C for H124L$^{C80-C116}$.

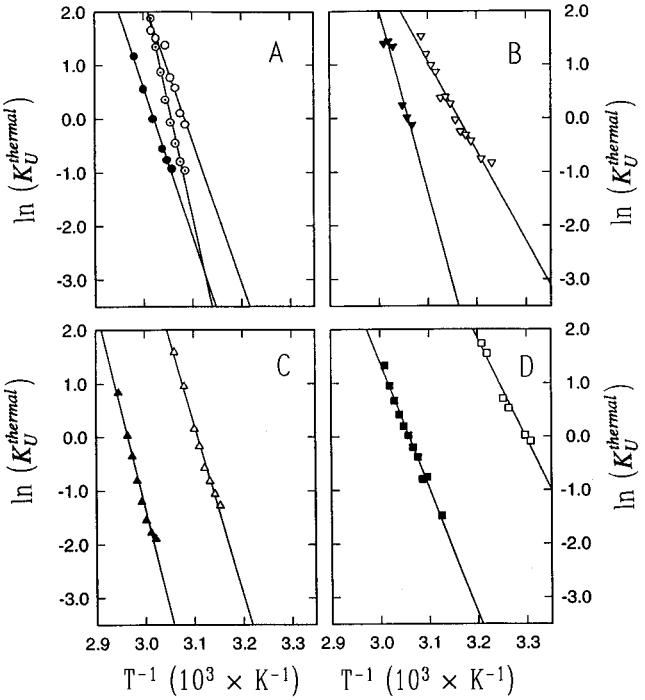

FIGURE 4: Thermodynamic van't Hoff plots of the two-state equilibrium unfolding constant (K_U^{NMR}) as determined by variable-temperature NMR for the four mutants of nuclease containing engineered disulfide bonds. Filled symbols in each graph correspond to data collected in the absence of a reducing agent; open symbols correspond to data collected in the presence of a 30-fold molar excess of DTT. The dotted symbols in panel A correspond to the parent protein (H124L). Graph A contains data for H124L$^{C80-C116}$ and H124L. Graph B contains data for G79S+H124L$^{C80-C116}$. Graph C contains data for H124L$^{C77-C118}$. Graph D contains data for H124L$^{C79-C118}$.

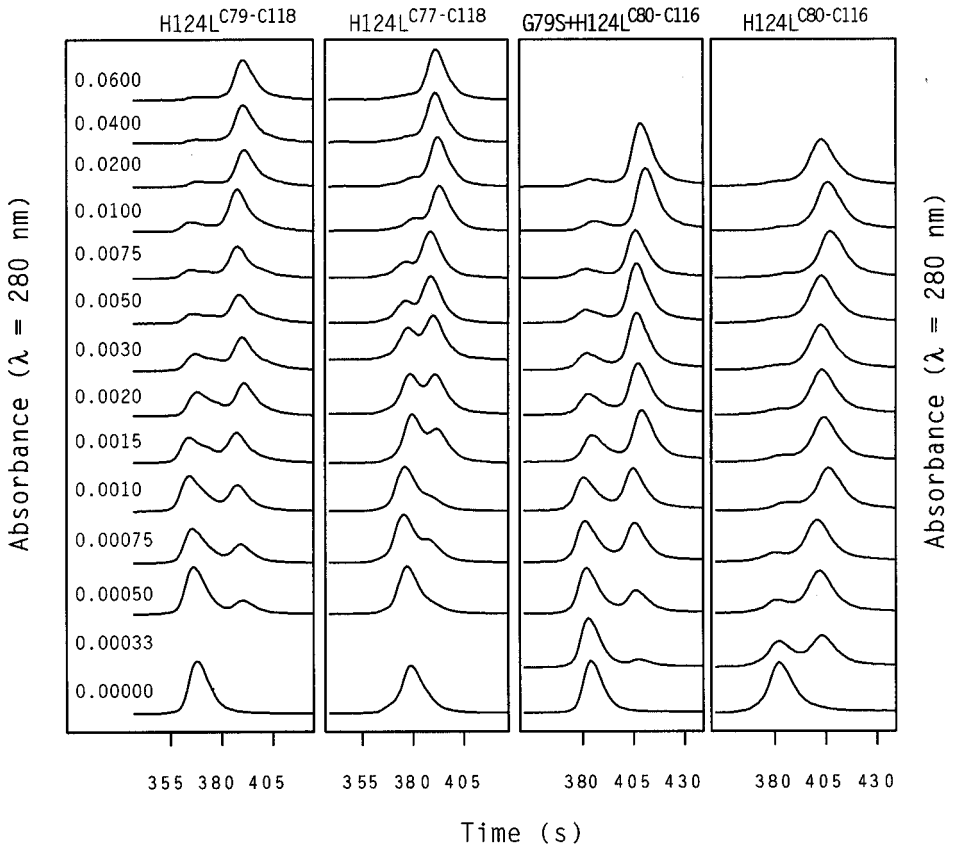

FIGURE 5: Separation of the reduced and oxidized forms of the disulfide mutants by reverse phase HPLC. Protein samples were incubated in solutions containing 10 mM potassium phosphate (pH 8.0) at different ratios of DTT_{SH}^{SH}/DTT_{S-S} included in buffer, as indicated in the left panel. The reaction was quenched by addition of acetic acid, and the component species were separated by chromatography on a C4 reverse phase column with a linear gradient ranging from 60:40 to 50:50 H_2O/CH_3CN, over a period of 8 min, at a flow rate of 1 mL/min.

Table 4: Equilibrium Reduction Constants Determined for the Engineered Disulfide Mutants of Nuclease H124L[a]

protein variant	K_{Red}^{F} [b]	ΔG_{Red}^{F} [c] (kcal mol^{-1})	n[d]	ΔG_{Red}^{U} [e] (kcal mol^{-1})	$\Delta\Delta G_{red}$ [f] (kcal mol^{-1})
$H124L^{C80-C116}$	4500 ± 1500	−5.0 ± 0.1	37	−3.79	−1.21
$G79S+H124L^{C80-C116}$	850 ± 310	−4.0 ± 0.3	37	−3.79	−0.21
$H124L^{C79-C118}$	480 ± 110	−3.7 ± 0.3	40	−3.86	0.16
$H124L^{C77-C118}$	390 ± 80	−3.5 ± 0.3	42	−3.90	0.40

[a] The samples were dissolved in 10 mM K_2HPO_4 at pH 8.0 and $T = 298$ K. [b] $K_{Red} = [DTT_{S-S}][protein_{SH}^{SH}]/[DTT_{SH}^{SH}][protein_{S-S}]$. [c] $\Delta G_{Red}^{F} = -RT \ln(K_{Red}^{F})$, and $T = 298$ K. [d] Loop size formed by disulfide bond (residues). [e] $\Delta G_{Red}^{U} = 294.5\ K[-2.1 - {}^{3}/_{2}R \ln(n)]$ (Pace et al., 1988). [f] $\Delta\Delta G_{Red} = \Delta G_{Red}^{F} - \Delta G_{Red}^{U}$.

Equilibrium Reduction Constants. Equilibrium constants for the reaction indicated by eq 7, K_{Red}^{F}, were measured by incubating each of the mutants in a buffer, at pH 7.0, containing a known concentration of DTT_{S-S} and DTT_{SH}^{SH}. The reaction was then quenched by the addition of acetic acid, and the nonreduced and reduced forms for each mutant were separated by reverse phase HPLC. Accurate estimates for K_{Red}^{F} were determined by measuring the ratio of the reduced and nonreduced forms as a function of the ratio of reduced to oxidized DTT included in the incubation buffer (Figure 5). The results (Table 4) show that K_{Red}^{F} differs by greater than a factor of 10 among the four mutants.

DISCUSSION

Thermodynamic Stability. The thermodynamic stability of disulfide-containing proteins can be analyzed in terms of the following four-state model

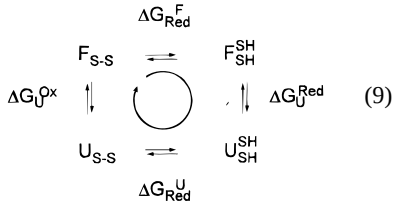

(9)

where F_{S-S} and F_{SH}^{SH} represent the oxidized and reduced forms of the folded protein and U_{S-S} and U_{SH}^{SH} represent the oxidized and reduced forms of the unfolded protein, respectively. Free energies for the unfolding reaction of the oxidized and reduced forms are given by ΔG_U^{Ox} and ΔG_U^{Red}, whereas those for the reduction reaction of the folded and unfolded forms are given by ΔG_{Red}^{F} and ΔG_{Red}^{U}. The four equilibria are coupled and reversible such that

$$\Delta G^{F}_{Red} + \Delta G^{Red}_{U} - \Delta G^{U}_{Red} - \Delta G^{Ox}_{U} = 0 \qquad (10)$$

Energies for folding/unfolding and oxidation/reduction can be separated and rewritten as

$$\Delta G^{F}_{Red} - \Delta G^{U}_{Red} = \Delta G^{Ox}_{U} - \Delta G^{Red}_{U} \qquad (11)$$

If we define $\Delta\Delta G_{Red}$ as $\Delta G^{F}_{Red} - \Delta G^{U}_{Red}$and $\Delta\Delta G_{U}$ as $\Delta G^{Ox}_{U} - \Delta G^{Red}_{U}$, eq 11 reduces to $\Delta\Delta G_{Red} = \Delta\Delta G_{U}$. Values for $\Delta\Delta G_{U}$ have been obtained by two independent methods, under different solution conditions, and are reported in Tables 2 and 3, respectively. On the basis of reduction data for the folded form of the protein (ΔG^{F}_{Red}, Table 4) alone, however, it is impossible to calculate $\Delta\Delta G_{Red}$ directly. Nevertheless, the chain entropy model explains the effects of engineered disulfide bonds in terms of a loop-length-dependent change in the entropy of the denatured state. Therefore, according to this model, the only contribution to ΔG^{U}_{Red} is given by

$$T\Delta S = T[-2.1 - {}^{3}/_{2}R \ln(n)] \qquad (12)$$

where n is the number of residues in the loop formed by the disulfide bond (Pace et al., 1988). The magnitude of the calculated $T\Delta S$ term for the 80−116, 79−118, and 77−118 disulfides at 294.5 K varies between −3.8 and −3.9 kcal mol^{-1} (Table 4). Predicted values of ΔG^{U}_{Red}, along with the measured values of ΔG^{F}_{Red}, provide the basis for our estimates of $\Delta\Delta G_{Red}$ (Table 4).

The current experimental results do not permit direct verification of eq 11 because $\Delta\Delta G_{Red}$ and $\Delta\Delta G_{U}$ were measured under different solution conditions. Nevertheless, comparisons of the experimentally determined $\Delta\Delta G_{U}$ values with our estimates of $\Delta\Delta G_{Red}$ for the four different mutants, as shown in Figure 6A,B, reveal that these quantities are positively correlated; plots of $\Delta\Delta G_{U}$ versus $\Delta\Delta G_{Red}$ (not shown) have correlation coefficients of 0.94 and 0.85, respectively, for the GdmCl and thermal unfolding data. These results are consistent with the expectation that the increase in stability attributed to disulfide formation is maximized when strain in the folded state [as judged by folded state reduction potentials (eq 8)] is minimized.

Since quantitative agreement with the four-state unfolding model has not been established, we cannot rule out alternative interpretations of the data presented here. For example, the positive correlation observed in Figure 6A,B could be somewhat misleading as we have assumed that ΔG^{U}_{Red} is determined solely by entropy terms that depend on the length of the loop created by the disulfides. Additional effects on the unfolded state, either entropic or enthalpic, might be present such that $\Delta\Delta G_{Red}$ becomes uncorrelated or negatively correlated with $\Delta\Delta G_{U}$. Although it is not possible to directly address this problem given the data presented here, we have used additional structural data, obtained by high-resolution NMR spectroscopy (discussed below), to show that the perturbation free energies for unfolding are correlated with a specific structural change in the folded state.

Disulfide-Induced Strain in the Folded State. Previous workers (Matsumura et al., 1989; Pace et al., 1988) have suggested that the introduction of strain in the folded state is as important as entropic/enthalpic effects in the unfolded state. In the present results, the coupling of disulfide formation to the perturbation of the *cis/trans* equilibrium toward the *trans* form has been used to quantitatively assess a particular form of strain energy. Conversely, coupling of disulfide formation to perturbation of the *cis/trans* equilibrium toward the *cis* form has been used to assess stabilizing folded state effects. Evidence to support this model follows from the results presented in Figure 6C,D, which demonstrate that the increase in stability that accompanies disulfide

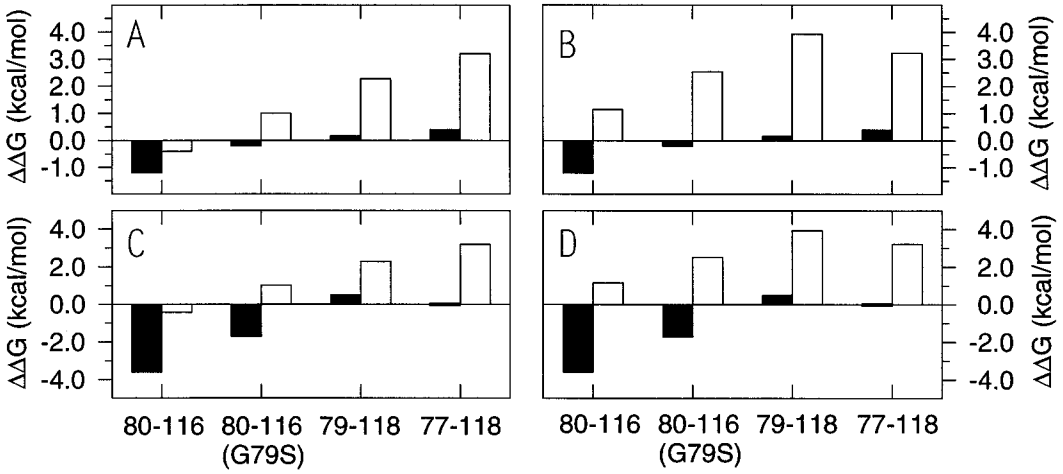

FIGURE 6: Relationships among the reduction potentials in the folded state (A and B), disulfide-induced changes in the *cis/trans* equilibrium at the Xxx^{116}−Pro^{117} peptide bond (C and D), and disulfide-induced changes in protein stability. The data are presented in pairs for each of the four mutants (indicated along the abscissa), with values for one of the perturbation free energies being indicated by solid bars and those for others by open bars. (A) Histogram that compares the differential reduction potential of the folded and unfolded states (solid) versus the differential stability of the oxidized and reduced forms as determined by GdmCl-induced protein unfolding (open). Linear fitting of the data reveals $\Delta\Delta G_{Red} = 0.44(\Delta\Delta G^{GdmCl}_{U}) - 0.87$ ($r^2 = 0.94$). (B) Histogram that compares the differential reduction potential of the folded and unfolded states (solid) versus the differential stability of the oxidized and reduced forms as determined by thermal unfolding experiments (open). Linear fitting of the data reveals $\Delta\Delta G_{Red} = 0.55(\Delta\Delta G^{NMR}_{U}) - 1.69$ ($r^2 = 0.85$). (C) Histogram that compares the perturbation of the *cis:trans* equilibrium for the Xxx^{116}−Pro^{117} peptide bond by covalent disulfide formation (solid) versus the differential stability of the oxidized and reduced forms as determined by GdmCl-induced protein unfolding (open). Linear fitting of the data reveals $\Delta\Delta G_{c/t} = 1.11$ ($\Delta\Delta G^{GdmCl}_{U}$) − 2.89 ($r^2 = 0.88$). (D) Histogram that compares the perturbation of the *cis:trans* equilibrium for the Xxx^{116}−Pro^{117} peptide bond by covalent disulfide formation (solid) versus the differential stability of the oxidized and reduced forms as determined by thermal unfolding experiments (open). Linear fitting of the data reveals that $\Delta\Delta G_{c/t} = 1.55$ ($\Delta\Delta G^{NMR}_{U}$) − 5.39 ($r^2 = 0.98$).

formation ($\Delta\Delta G_U^{GdmCl}$ or $\Delta\Delta G_U^{thermal}$) is positively correlated to the free energy change ($\Delta\Delta G_{c/t}$) for the *cis/trans* transition at the 116−117 peptide bond. Relative to the configuration favored under reducing conditions, an engineered disulfide that shifts the *cis/trans* equilibrium toward the *trans* form diminishes the stabilizing effect of disulfide. Plots of $\Delta\Delta G_U$ versus $\Delta\Delta G_{c/t}$ (not shown) reveal that these quantities are strongly correlated, with a slope of 1.1 and 1.5 for the GdmCl and thermal unfolding data, respectively. This suggests that the *cis/trans* perturbation reports in a nearly quantitative fashion on the particular form of strain energy present in the engineered disulfides considered here. Errors in estimates of $K_{c/t}$ for those mutants in which $K_{c/t}$ was strongly perturbed, differences in solution conditions under which the data were collected, and a strong temperature dependence of these equilibria which has been neglected may each contribute to the differences in the slopes observed.

Cis Pro^{117} of Staphylococcal Nuclease. The coupling of disulfide bond formation to perturbation of the *cis/trans* equilibrium for isomerization of the Xxx^{116}−Pro^{117} peptide bond is best understood by reference to the model proposed by Hodel et al. (1993). This model, which describes important parameters that determine the *cis/trans* equilibrium, postulates that the loop from Ala^{112} to Asn^{118} containing the type VI$_a$ β turn containing Pro^{117} is anchored near its ends. At the N-terminal end of the loop, packing interactions dominate, and at the C-terminal end, hydrogen-bonding interactions dominate. Anchorage of the ends of the loop in a specific orientation results in the introduction of differential strain that depends on the configurational state (*cis* or *trans*) of the the Xxx^{116}−Pro^{117} peptide bond. In the wild-type protein, this perturbs the equilibrium to the otherwise less favorable *cis* configuration. Two important corollaries of this model, which have not been emphasized by the Fox group, are (1) that specific interactions, within the protein but outside the loop containing Pro^{117}, must be responsible for the positioning and stabilization of the anchorage positions and (2) that any strain in the loop thus must be transmitted back to the rest of the protein and will serve to weaken the interactions responsible for proper anchorage. This extended model explains how substitutions remote from the loop, for example, substitutions at residue 124 (Truckses et al., 1996), can influence $K_{c/t}$. Finally, the mutual interaction between the loop and the rest of the protein can be decoupled by mutations, such as P117G, that introduce flexibility into the loop; the stabilization of this particular mutation can be explained by the removal of strain transmitted from the loop to the rest of the protein when Pro^{117} is present (Truckses et al., 1996).

Mutations at residue 124 that increase the global stability of the protein also lead to an increase in $K_{c/t}$; however, the effect is loosely coupled (a 1 kcal increase in stability is associated with only a 0.17 kcal perturbation in $K_{c/t}$) (Truckses et al., 1996). By contrast, the stabilizing effects of the disulfide mutants studied here (Figure 6C,D) are nearly fully coupled to the change in $K_{c/t}$ (a 1 kcal increase in stability is associated with a 0.6−0.9 kcal perturbation in $K_{c/t}$). This suggests that the effect of the engineered disulfides on protein stability is correlated with their ability to lock Pro^{117} into a configuration in a way that either reinforces or modulates interactions elsewhere in the protein. Clearly, the determination of detailed three-dimensional structures of the oxidized and reduced forms of these mutants is the next step toward understanding the mechanism by which the isomeric state of the Xxx^{116}−Pro^{117} peptide bond is coupled to disulfide formation.

Inferences for Protein Engineering. The set of four mutants designed and tested here can be considered only marginally successful in terms of engineered stability; only one of them displayed a free energy value for unfolding higher than that of the wild-type protein. What the results clearly show, however, is that native state effects can profoundly modulate the extent of successful stabilization and that the introduction of a disulfide bond can lead to the enhancement of existing folded state interactions (e.g., H124L$^{C80-C118}$) in cases where unfavorable native state effects can be eliminated.

ACKNOWLEDGMENT

The authors thank Dr. Catherine Royer (University of Wisconsin School of Pharmacy), who generously provided facilities for carrying out the fluorimetry experiments, Dr. Hong Cheng (now at the Fox Chase Cancer Center), who provided useful advice regarding synthesis of ^{13}C-labeled cystine, and Dr. Janet Wood (University of Guelph, Guelph, Ontario), who provided the proC Δ(*putPA*) strain of *E. coli*.

SUPPORTING INFORMATION AVAILABLE

Two tables which present the data from DTNB and steady state kinetics experiments, respectively, one figure which demonstrates the identification of prolyl−peptide bond configurations by isotope-filtered two-dimensional NOE spectroscopy, and reaction schemes which outline the preparation of [$^{13}C^{\alpha}$, $^{13}C^{\alpha\prime}$]-D,L-cystine (6 pages). Ordering information is given on any current masthead page.

REFERENCES

Alexandrescu, A. T., Mills, D. A., Ulrich, E. L., Chinami, M., & Markley, J. L. (1988) *Biochemistry 27*, 2158−2165.
Alexandrescu, A. T., Hinck, A. P., & Markley, J. L. (1990) *Biochemistry 29*, 4516−4525.
Anfinsen, C. B., & Sheraga, H. A. (1975) *Adv. Protein Chem. 29*, 205−299.
Atkinson, R. O., Poppelsdorf, F., & Williams, G. (1953) *J. Chem. Soc.*, 580−581.
Betz, S. F. (1993) *Protein Sci. 2*, 1551−1558.
Bundi, A., & Wüthrich, K. (1979) *Biopolymers 18*, 285−297.
Carra, J. H., & Privalov, P. L. (1995) *Biochemistry 34*, 2034−2041.
Carra, J. H., Anderson, E. A., & Privalov, P. L. (1994) *Biochemistry 33*, 10842−10850.
Cheng, H. (1990) Ph.D. Thesis, Hunter College, New York.
Clarke, J., & Fersht, A. R. (1993) *Biochemistry 32*, 4322−4329.
Cooper, A., Eyles, S. J., Radford, S. E., & Dobson, C. M. (1992) *J. Mol. Biol. 225*, 939−943.
Cotton, F. A., Hazen, E. E., Jr., & Legg, M. J. (1979) *Proc. Natl. Acad. Sci. U.S.A. 76*, 2551−2555.
Creighton, T. E. (1974) *J. Mol. Biol. 87*, 579−602.
Creighton, T. E. (1988) *Bioessays 8*, 57−63.
Cuatrecasas, P., Fuchs, S., & Anfinsen, C. B. (1967) *J. Biol. Chem. 242*, 1541−1547.
Dill, K. A. (1990) *Biochemistry 29*, 7133−7155.
Doig, A. J., & Williams, D. H. (1991) *J. Mol. Biol. 217*, 389−398.
Evans, P. A., Dobson, C. M., Kautz, R. A., Hatfull, G., & Fox, R. O. (1987) *Nature 329*, 266.
Evans, P. A., Kautz, R. A., Fox, R. O., & Dobson, C. M. (1989) *Biochemistry 28*, 362−370.
Flory, P. J. (1956) *J. Am. Chem. Soc. 78*, 5255−5235.

Green, S. M., Meeker, A. K., & Shortle, D. (1992) *Biochemistry 31*, 5717−5728.
Grissom, C. B., & Markley, J. L. (1989) *Biochemistry 28*, 2116−2124.
Hinck, A. P. (1993) Ph.D. Thesis, University of Wisconsin, Madison, WI.
Hinck, A. P. Loh, S. N., Wang, J., & Markley, J. L. (1990) *J. Am. Chem. Soc 112*, 9031−9034.
Hinck, A. P., Eberhardt, E. S., & Markley, J. L. (1993) *Biochemistry 32*, 11810−11818.
Hodel, A., Kautz, R. A., Jacobs, M. D., & Fox, R. O. (1993) *Protein Sci. 2*, 838−850.
Hodel, A., Kautz, R. A., & Fox., R. O. (1994) *Protein Sci. 3*, 549−556.
Hodel, A., Kautz, R. A., & Fox, R. O. (1995) *Protein Sci. 4*, 484−495.
Hynes, T. R., & Fox, R. O. (1991) *Proteins: Struct., Funct., Genet. 10*, 92−105.
Jocelyn, P. C. (1987) *Methods Enzymol. 143*, 43−66.
Kuroki, R., Inaka, K., Taniyama, Y., Kidokoro, S., Matsushima, M., Kikuchi, M., & Yutani, K. (1992) *Biochemistry 31*, 8323−8328.
Loh, S. N. (1993) Ph.D. Thesis, University of Wisconsin, Madison, WI.
Loh, S. N., & Markley, J. L. (1994) *Biochemistry 33*, 1029−1036.
Loh, S. N., McNemar, C. W., & Markley, J. L. (1991) in *Techniques in Protein Chemistry II* (Villafranca, J. J., Ed.) pp 275−282, Academic Press, New York.
Loll, P. J., & Lattman, E. E. (1989) *Proteins: Struct. Funct. Genet., 5*, 183−201.
Matsumura, M., Becktel, W. J., Levitt, M., & Matthews, B. W. (1989) *Proc. Natl. Acad. Sci. U.S.A. 86*, 6562−6566.
Mitchison, C., & Wells, J. A. (1989) *Biochemistry 28*, 4807−4815.
Pace, C. N. (1975) *Crit. Rev. Biochem. 3*, 1−43.
Pace, C. N., Grimsley, G. R., Thomson, J. A., & Barnett, B. J. (1988) *J. Biol. Chem. 263*, 11820−11825.
Poland, D. C., & Sheraga, H. A. (1965) *Biopolymers 3*, 379−399.
Raleigh, D. P., Evans, P. A., Pitkeathly, M., & Dobson, C. M. (1992) *J. Mol. Biol. 228*, 338−342.
Royer, C. A., Hinck, A. P., Loh, S. N., Prehoda, K. E., Peng, X., Jonas, J., & Markley, J. L. (1993) *Biochemistry 32*, 5222−5232.
Saunders, A. J., Young, G. B., & Pielak, G. J. (1993) *Protein Sci. 2*, 1183−1184.
Schellman, J. A. (1978) *Biopolymers 17*, 1305−1322.
Shortle, D. (1983) *Gene 22*, 181−189.
Shortle, D., & Meeker, A. K. (1986) *Proteins: Struct., Funct., & Genet. 1*, 81−89.
Shortle, D., Stites, W. E., & Meeker, A. K. (1990) *Biochemistry 29*, 8033−8041.
Sondek, J., & Shortle, D. (1990) *Proteins: Struct., Funct., Genet. 7*, 299−305.
Tanuichi, H., Anfinsen, C. B., & Sodja, A. (1967) *J. Biol. Chem. 242*, 4752−4758.
Thornton, J. A. (1981) *J. Mol. Biol. 151*, 261−287.
Tidor, B., & Karplus, M. (1993) *Proteins: Struct., Funct., Genet. 15*, 71−79.
Torchia, D. A., Sparks, S. W., Young, P. E., & Bax, A. (1989a) *J. Am. Chem. Soc. 111*, 8315−8317.
Torchia, D. A., Sparks, S. W., & Bax, A. (1989b) *Biochemistry 28*, 5509−5524.
Truckses, D. M., Somoza, J., Prehoda, K. E., & Markley, J. L. (1996) *Protein Sci.* (in press).
Wang, J. F., LeMaster, D. M., & Markley, J. L. (1990a) *Biochemistry 29*, 88−101.
Wang, J. F., Hinck, A. P., Loh, S. N., & Markley, J. L. (1990b) *Biochemistry 29*, 4242−4253.
Wang, J. F., Hinck, A. P., Loh, S. N., & Markley, J. L. (1990c) *Biochemistry 29*, 102−113.
Wells, J. A., & Powers, D. B. (1986) *J. Biol. Chem. 261*, 6564−6570.
Wetzel, R., Perry, L. J., Baase, W. J., & Becktel, W. J. (1987) *Proc. Natl. Acad. Sci. U.S.A., 85*, 401−405.
White, S. H. (1992) *J. Mol. Biol. 227*, 991−995.
Wüthrich, K. (1986) *NMR of Proteins & Nucleic Acids*, Wiley, New York.

BI960309O